WWJMRD 2024; 10(03): 39-47
www.wwjmrd.com
International Journal
Peer Reviewed Journal
Refereed Journal
Indexed Journal
Impact Factor SJIF 2017: 5.182 2018: 5.51, (ISI) 2020-2021: 1.361
E-ISSN: 2454-6615

Blaise Ngwem Bayiha
Department of Civil Engineering, Advanced Technical Teacher Training College of the Technical education, The University of Douala, Douala, Cameroon.

Benjamin Bahel
Laboratory of Energy Modeling Materials and Methods (E3M); National Higher Polytechnic School of Douala, The University of Douala, Douala, Cameroon.

Fabien Kenmogne
Department of Civil Engineering, Advanced Teacher Training College of the Technical education, The University of Douala, Douala, Cameroon.

André Abanda,
Arnaud Kamdem Takungang,
Jean Chills Amba,
Laboratory of Energy Modeling Materials and Methods (E3M); National Higher Polytechnic School of Douala, The University of Douala, Douala, Cameroon.

Correspondence:
Blaise Ngwem Bayiha
Department of Civil Engineering, Advanced Technical Teacher Training College of the Technical education, The University of Douala, Douala, Cameroon.

Investigation of Young modulus of concrete with partial substituting of the ordinary Portland cement with metakaolin: Application with Cameroonian CEM I cement

Blaise Ngwem Bayiha, Benjamin Bahel, Fabien Kenmogne, André Abanda, Arnaud Kamdem Takungang, Jean Chills Amba

Abstract
This paper deals with the prediction of Young modulus of concrete obtained with partial substitution of ordinary portland cement with metakaolin. A multiple time scale approach is then applied on two models based on micromechanics with the aim to homogenise the obtained Young modulus. The homogenisation schemes involved here are the self-consistency and Mori-Tanka ones. According to the Mori-Tanaka scheme, various shapes of inclusion are considered in the model, and the products of the pozzolanic reaction are taken into account at the appropriate scale. In order to justify the robustness of our analytical findings, the predicted results is compared to experimental observations on ordinary concrete with metakaolin as partial substitute of CEM I, cement. Moreover, we found experimentally that there is an optimal rate of substitution above which further substitution has an adverse effect. As results, the model involving the self-consistency scheme predicts values closed to that found experimentally, while for the scheme of Mori-Tanaka, the values predicted are closed to that found experimentally if both the shape of all the inclusions phases are considered spherical, or the void inclusion phases are considered ellipsoidal.

Keywords: Metakaolin; self-consistency; Mori-Tanaka; prediction; Young modulus

1. Introduction

About a decade ago, remarkable advances have taken place in the research on supplementary materials that can be used as partial substitution of Portland cement, the well-known cement substitutes [1, 2]. Cement substitutes are materials that may be substituted, to some degree, in order to improve different properties, such as strength and durability [1]. The use of cement substitutes is generally encouraged because of the environmental advantages gained from their diversion from the waste stream, the reduction of the energy required in their re-purposing as compared to the manufacture of cement. However, much greenhouse gas is created during the production of cement among which Carbon dioxide (CO_2). It has been proven that cement industry produces about 7% of global CO_2 emission [3]. This is why over the past few years the interest in reducing the CO_2 footprint of the material has increased, primarily by lowering the amount of cement via use of supplementary cementious materials.
Supplementary cementious materials are used to reduce the clinker factor of cements. It has been proven that some of these materials over a particular value of rate, namely the threshold, can reduce the mechanical properties of concretes, particularly at early age[4], which is not suitable. Recent studies have been conducted on the use of metakaolin in concrete as supplementary cementious material, particularly due to the fact that it demonstrated excellent pozzolanic properties (See [4] and references therein). To name just a few, Deteuf [2] proposed that metakaolin reacts with the CH available from the hydration reaction of cement to form more CSH gel and a crystallised product (C_2ASH_8). In the same light, Wild [3] showed that for the same reaction, two additional crystallized products are formed (C_4AH_{13} and C_3AH_6). It has been proven that factors like types of cement, AS_2/CH

ratio and temperature affect the reaction between metakaolin and CH [5]. Let us mention that distinct crystallised products are formed with the CSH gel when the AS2/CH ratio reaches a specific value.

Numerous experimental studies have been carried out on concrete with partial substitution of ordinary Portland cement with supplementary cementious materials [6,7,8]. Concomitantly, models for predictions of their elastic properties have been proposed [9,10]. While the approach used there were similar to that proposed by Zadeh and Bobko [11]. A multi-scale approach was used to predict elastic properties of concrete with metakaolin by applying the self-consistency and Mori-Tanaka scheme at four scales[12], and by taking into account the products of the pozzolanic reaction, agreeing then with the works of Wild [3] and Amer et al [9] in order to account for the change in elastic properties. Nazargah et al [13] showed that, for single scale predictions, the shape of the inclusion phase influences the quality of the predictions obtained. *One may wonder whether the taking into account non-spherical shapes for inclusion phases can permit to have some mechanical properties of concrete such as Young modulus obtained by progressively substitute ordinary Portland cement with metakaolin.* It has been proven that mechanical and physical performances of concretes are affected by geological nature of sand, the place and temperature of the locality where experiments are performed [14]. At this stage, the query is to know at *what percentage the metakaolin could ameliorate the mechanical properties of concretes in general and particularly in Cameroon*? Limiting our scope to the metakaolin used in this work. The main objective of this work is to propose a model that can predict the young modulus of concrete with partial substitution of cement with locally available metakaolin, considering pozzolanic reaction and the non-spherical shapes of inclusion phases of the concrete.

2. Multiscale material model for Young's modulus

2.1. Observation scales and modelling of microstructure

Four scales of studies are used here, while the homogenisation schemes are applied at each scale to obtain the effective elastic properties of the resulting concrete. These scales used include:

- Scale 1(from 10-8 to 10-6m) for which two types of CSH gel can be observed namely; LD CSH and HD CSH[15]. These phases are considered as spherical inclusion [16].
- At scale 2 (going from 10^{-6} to 10^{-4}m), the products of the hydration and pozzolanic reactions can be observed, leading to the inclusion phases: The unreacted clinker, metakaolin, CH, pores and the crystallised phases (C_4AH_{13}, C_3AH_6 and C_2ASH_8) [16]. The CSH gel is matrix phase.
- At scale 3(from 10^{-4} to 10^{-2}m), the inclusion phases are sand and void phases and the matrix phase is the cement paste.
- Finally at scale 4(As from 10^{-2}m), the inclusion phases are small and coarse gravel. The matrix phase is the mortar. In this stage, the ITZ is not considered according to works of Zadeh and Bobko [11] proving that for models predicting elastic properties, it can be ignored.

2.2. Homogenisation scheme

To obtain the effective elastic properties of heterogeneous materials, we propose an equivalent homogenous material with a constant Young modulus. This is done in three steps namely: the representation, the localisation and the homogenisation.

- Representation: Here, the representative volumetric element is mathematically defined and some assumptions made:
  - The representative volumetric element represents globally all elementary volumes;
  - Let us consider that the region studied is statistically homogenous [17], meaning the n- point correlation function of its characteristic function, $f_i(x,\alpha)$ is such as

$$P_{r1,\dots,rn}\left(x,x',\dots,x'^{n-1}\right) =< f_{r1}(x,\alpha) >< f_{r2}(x',\alpha) > \cdots < f_{rn}\left(x'^{n-1},\alpha\right) >= \int_v f_{r1}(x,\alpha) f_{r2}(x',\alpha) \dots f_{rn}\left(x'^{n-1},\alpha\right) p(\alpha) dm \quad (1)$$

is insensitive to translation.

-The ergodic hypothesis next is assumed, meaning that the ensemble average is closed to that of the volume average. The mean of a physical property $\langle \Phi \rangle$ of the microstructure in a small volume V is defined as:

$$\langle \Phi \rangle = \bar{\Phi} = \lim_{x\to\infty} \frac{1}{V} \int_v \Phi(x)\, dv \quad (2)$$

- Localisation: the dependency between the physical quantities at both microscopic and macroscopic scales is established. Additionally, the boundary conditions on the representative volumetric element are proposed as:

$$(\sigma_{ij} - \sigma_{ij}^0) n_j = 0, \quad (3)$$

for homogenous stress. Where σ_{ij}^0 is the overall stress tensor causing strain, while the global stress is

$$\langle \sigma_{ij}(x) \rangle = \overline{\sigma_{ij}} = \frac{1}{V} \int \sigma_{ij}(x)\, dv = \sum_{r=1}^{n} c_r \sigma_{ij}^r . \quad (4)$$

σ_{ij}^r being the mean stress of a phase in the total volume v_r, while c_r is the volume fraction of a phase. Using the constitutive laws on the mean stress in each phase, one has $\sigma_{ij}^r(x) = C_{ijkl}^r \varepsilon_{kl}^r$ leading to

$$\overline{\sigma_{ij}} = \sum_{r=1}^{n} c_r \sigma_{ij}^r = \sum_{r=1}^{n} c_r C_{ijkl}^r \varepsilon_{kl}^r . \quad (5)$$

The relationship between the mean strain field in a sub-volume and the strain field causing it is defined as

$$\varepsilon_{ij}^r = A_{ijkl}^r(x) \varepsilon_{kl}^o, \quad (6)$$

where the tensor A_{ijkl}^r is the mechanical strain concentration factor tensor [17].

- Homogenisation: The effective constitutive laws are determined from the local constitutive laws. The mean global stress here is expressed as:

$$\overline{\sigma_{ij}} = \sum_{r=1}^{n} c_r C_{ijkl}^r \bar{\varepsilon}_{kl}^r = \sum_{r=1}^{n} c_r C_{ijkl}^r A_{klmn}^r \bar{\varepsilon}_{mn}^o . \quad (7)$$

By setting $\overline{\sigma_{ij}} = C_{ijkl} \varepsilon_{kl}^o$, one has the following definition:

$$C_{ijkl} = \sum_{r=1}^{n} c_r C_{ijmn}^r A_{mnkl}^r . \quad (8)$$

The relationship between local stress, ε_{ij}^r, in a sub-volume and the eigenstrain, μ_{ij}^r, in the sub-volume, which is the strain field not resulting from mechanical loading applied (see [17]), is

$$\varepsilon_{ij}^r = S_{ijkl} \mu_{kl}^r(x). \quad (9)$$

S_{ijkl} being the Eshelby tensor, which describes the effect of an inclusion on the local strain field. To account for the change in properties when considering the inclusion, the stress is considered as

$$\sigma_{ij}^r(x) = \sigma_{ij}^0 + \sigma_{ij}^{pt}(x) \quad (10)$$

where

$$\sigma_{ij}^r(x) = \begin{cases} C_{ijkl}^r\left[\varepsilon_{kl}^0 + \varepsilon_{kl}^{pt}(x)\right] & x \in \Omega \\ C_{ijkl}\left[\varepsilon_{kl}^0 + \varepsilon_{kl}^{pt}(x)\right] & x \in V - \Omega \end{cases} \quad (11)$$

is the perturbation stress field with respect to the macroscopic stress, Ω and V the volumes of both the inclusions and the composite studied. This problem will be solved by considering both the superposition of the situation with the uniform inclusion without eigenstrain under ε_{ij}^0 strain field and that when the uniform inclusion under eigenstrain μ_{ij}^r is without overall loading [17], leading Eq.(10) to

$$\sigma_{ij}^r(x) = \begin{cases} C_{ijkl}^r[\varepsilon_{kl}^0 + \varepsilon_{kl}^r(x) - \mu_{kl}^r(x)] & x \in \Omega \\ C_{ijkl}\left[\varepsilon_{kl}^0 + \varepsilon_{kl}^{pt}(x)\right] & x \in V - \Omega \end{cases} \quad (12)$$

By combining Eqs.(8), and (11), it is obvious that

$$\mu_{ij}^r = \left[\left(C_{ijkl} - C_{ijkl}^r\right)S_{klmn} + C_{ijmn}\right]^{-1}\left(C_{mnop}^r - C_{mnop}\right)\varepsilon_{op}^0 \quad (13)$$

❖ Self-consistency scheme

This scheme is considered in each sub-volume that solitary inclusions are embedded in the homogenised composite [17]. The local strain is given by $\varepsilon_{ij}^r = \varepsilon_{ij}^0 + S_{ijkl}\mu_{kl}^r$, leading from Eq.(12) to

$$\varepsilon_{ij}^r = \varepsilon_{ij}^0 + S_{ijkl}\left[(C_{klmn} - C_{klmn}^r)S_{mnop} + C_{mnop}\right]^{-1}\left(C_{opqr}^r - C_{opqr}\right)\varepsilon_{qr}^0 \quad (14)$$

Since $\varepsilon_{ij}^r = A_{ijkl}^r\varepsilon_{kl}^0$, one has

$$A_{ijkl}^r = \left[I_{ijkl} + S_{ijmn}C_{mnop}^{-1}(C_{opkl}^r - C_{opkl})\right]^{-1}, \quad (15)$$

from where the effective stiffness tensor is $C_{ijkl} = \sum_{r=1}^n c_r C_{ijmn}^r A_{mnkl}^r$, and can be rewritten as:

$$C_{ijkl} = C_{ijkl}^0 + \sum_{r=1}^n c_r(C_{ijmn}^r - C_{ijmn}^0)A_{mnkl}^r \quad (16)$$

❖ Mori-Tanaka scheme

This scheme is considered in each sub-volume that inhomogeneities are embedded in the matrix phase [17]. The global strain then can be written as

$$\varepsilon_{ij}^o = \sum_{r=1}^n c_r\overline{\varepsilon_{ij}^r} = \left(\sum_{r=1}^n c_r T_{ijkl}^r\right)\varepsilon_{kl}^1, \quad (17)$$

where the tensor T_{ijkl}^r is the partial mechanical strain concentration factor of the inhomogeneity. Let us set

$$T_{ijkl}^r = \left[I_{ijkl} + P_{ijmn}(C_{mnkl}^r - C_{mkl}^o)\right]^{-1}, \quad (18)$$

then the concentration tensor is written as:

$$\varepsilon_{ij}^1 = \left[\sum_{r=1}^n c_r T_{ijkl}^r\right]^{-1}\varepsilon_{kl}^o. \quad (19)$$

However

$$T_{ijkl}^1\varepsilon_{kl}^1 = \varepsilon_{ij}^1. \quad (20)$$

The combination of the above equations can lead to the following equation

$$\varepsilon_{ij}^r = T_{ijmn}^r[\sum_{s=1}^n c_s T_{mnkl}^s]^{-1}\varepsilon_{kl}^o. \quad (21)$$

From where it is obvious that:

$$A_{ijkl}^r = T_{ijmn}^r[\sum_{s=1}^n c_s T_{mnkl}^s]^{-1}, \quad (21)$$

leading to the effective stiffness tensor

$$C_{ijkl} = \left[\sum_{r=1}^n c_r\left(C_{ijmn}^r\right)T_{mnop}^r\right]\left[\sum_{s=1}^n c_s T_{opkl}^s\right]^{-1}. \quad (22)$$

The homogenisation schemes are used in their tensor form since some inclusion's phases will be considered ellipsoidal in shape. Additionally, the proposed generalised Mori-Tanaka scheme (see [18]) is not used due to the fact that the inclusions phases are not considered concentric. Instead, they are considered as distinct in space at each scale as shown in fig. 1. Some inclusion phases are supposed to be spherical and ellipsoidal with various eccentricities. The Eshelby tensor components for spherical and ellipsoidal shapes are given as follows:

- For spherical inclusions (see [18]), the components of tensor S_{ijkl} are defined as

$$S_{ijkl} = \frac{(5\vartheta-1)\delta_{ij}\delta_{kl}}{15(1-\vartheta)} + \frac{(4-5\vartheta)(\delta_{ik}\delta_{jl}+\delta_{il}\delta_{jk})}{15(1-\vartheta)}, \quad (23)$$

which can be given in extended form as:

$$S_{1111} = S_{2222} = S_{3333} = \frac{(7-5\vartheta)}{15(1-\vartheta)}, \quad (24)$$

$$S_{1122} = S_{1133} = S_{2233} = \frac{(5\vartheta-1)}{15(1-\vartheta)}, \quad (25)$$

$$S_{1212} = S_{2323} = S_{3131} = \frac{(4-5\vartheta)}{15(1-\vartheta)}. \quad (26)$$

For ellipsoidal inclusion with the constraints on x, y and z coordinates, respectively such as $a_1 > a_2 > a_3$[18], one can have the permutations as defined in Table 1, in which $I_2 = 4\pi - I_1 - I_3$, while I_1 and I_3 are defined as:

$$I_1 = \frac{4\pi a_1 a_2 a_3}{(a_1^2-a_2^2)(a_1^2-a_3^2)^{1/2}}[F(\theta,K) - E(\theta,K)], \quad (27)$$

$$I_3 = \frac{4\pi a_1 a_2 a_3}{(a_2^2-a_3^2)(a_1^2-a_3^2)^{1/2}}\left[\frac{a_2(a_1^2-a_3^2)^{1/2}}{a_1 a_3} - E(\theta,K)\right]. \quad (28)$$

where $F(\theta,K)$ and $E(\theta,K)$ are elliptic integral of the first and second kinds [19], respectively, with

$$\theta = \sin^{-1}\sqrt{\frac{a_1^2-a_3^2}{a_1^2}}, K = \sqrt{\frac{a_1^2-a_2^2}{a_1^2-a_3^2}}. \quad (29)$$

The other components being obtained from the following set of equations:

Table 1: Components of the Eshelby tensor.

Type of permutation applied	Coefficient of S	Values
	$S_{1111} =$	$\frac{3a_1^2}{8\pi(1-\vartheta)}I_{11} + \frac{(1-2\vartheta)}{8\pi(1-\vartheta)}I_1$
$1 \to 2$	$S_{2222} =$	$\frac{3a_2^2}{8\pi(1-\vartheta)}I_{22} + \frac{(1-2\vartheta)}{8\pi(1-\vartheta)}I_2$
$2 \to 3$	$S_{3333} =$	$\frac{3a_3^2}{8\pi(1-\vartheta)}I_{33} + \frac{(1-2\vartheta)}{8\pi(1-\vartheta)}I_3$
	$S_{1122} =$	$\frac{a_2^2}{8\pi(1-\vartheta)}I_{12} + \frac{(1-2\vartheta)}{8\pi(1-\vartheta)}I_1$

$1 \to 2,\ 2 \to 3$		$\frac{a_3^2}{8\pi(1-\vartheta)} I_{23} + \frac{(1-2\vartheta)}{8\pi(1-\vartheta)} I_2$
$2 \to 1,\ 3 \to 1$	$S_{3311} =$	$\frac{a_3^2}{8\pi(1-\vartheta)} I_{31} + \frac{(1-2\vartheta)}{8\pi(1-\vartheta)} I_3$
	$S_{1133} =$	$\frac{a_3^2}{8\pi(1-\vartheta)} I_{13} + \frac{(1-2\vartheta)}{8\pi(1-\vartheta)} I_1$
$1 \to 2,\ 3 \to 1$	$S_{2211} =$	$\frac{a_1^2}{8\pi(1-\vartheta)} I_{21} + \frac{(1-2\vartheta)}{8\pi(1-\vartheta)} I_2$
$2 \to 3,\ 1 \to 2$	$S_{3322} =$	$\frac{a_2^2}{8\pi(1-\vartheta)} I_{32} + \frac{(1-2\vartheta)}{8\pi(1-\vartheta)} I_3$
	$S_{1212} =$	$\frac{(a_1^2+a_2^2)}{16\pi(1-\vartheta)} I_{12} + \frac{(1-2\vartheta)}{8\pi(1-\vartheta)} (I_1+I_2)$
$1 \to 2,\ 2 \to 3$	$S_{2323} =$	$\frac{(a_2^2+a_3^2)}{16\pi(1-\vartheta)} I_{12} + \frac{(1-2\vartheta)}{8\pi(1-\vartheta)} (I_2+I_3)$
$2 \to 3,\ 3 \to 1$	$S_{3131} =$	$\frac{(a_3^2+a_1^2)}{16\pi(1-\vartheta)} I_{31} + \frac{(1-2\vartheta)}{8\pi(1-\vartheta)} (I_3+I_1)$

$$\begin{cases} 3I_{12} = \frac{(I_2-I_1)}{(a_1^2-a_2^2)}, \\ 3I_{11} + I_{12} + I_{13} = \frac{4\pi}{a_1^2}, \\ 3a_1^2 I_{11} + a_2^2 I_{12} + a_3^2 I_{13} = 3I_1, \end{cases} \quad (30)$$

$$\begin{cases} 3I_{23} = \frac{(I_3-I_2)}{(a_2^2-a_3^2)} \\ 3I_{22} + I_{23} + I_{21} = \frac{4\pi}{a_2^2} \\ 3a_2^2 I_{22} + a_3^2 I_{23} + a_1^2 I_{21} = 3I_2 \end{cases} \quad (31)$$

$$\begin{cases} 3I_{31} = \frac{(I_1-I_3)}{(a_3^2-a_1^2)}, \\ 3I_{33} + I_{31} + I_{32} = \frac{4\pi}{a_3^2}, \\ 3a_3^2 I_{33} + a_1^2 I_{31} + a_2^2 I_{32} = 3I_3. \end{cases} \quad (32)$$

The homogenisation schemes are then applied on each scale of consideration to homogenise the phases observed. This approach results in the effective elastic properties of concrete with metakaolin.

3. Method

We applied homogenization schemes at each given scale under consideration to obtain the elastic properties of the matrix phase in the next scale of consideration:

3.1 Scale 1:

The self-consistency scheme is applied for model 1 and 2 to obtain the elastic properties of the CSH gel which is the matrix phase in scale 2.. The elastic properties and volume fraction used for the two inclusion phases (LD CSH and HD CSH) are obtained from previous experimental studies [15, 16]. The inclusion phases are considered spherical [16].

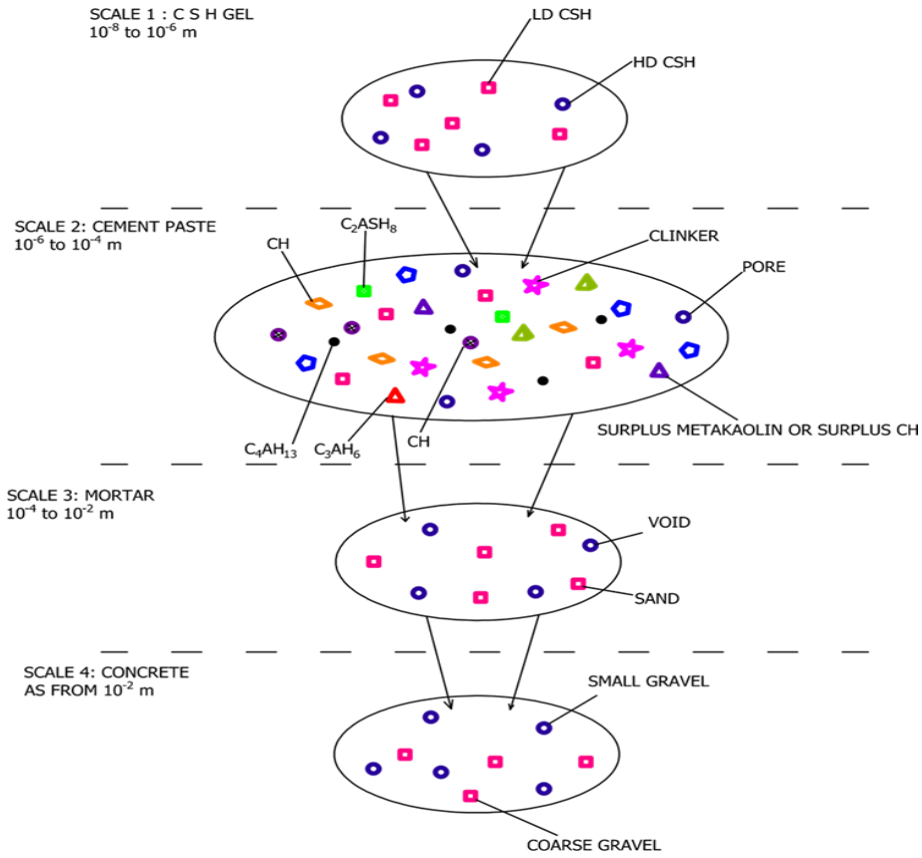

Fig. 1: Illustration of the four scales model

3.2 Scale 2

The Self-consistency scheme is applied for model 1 and the Mori-Tanaka is the applied scheme for model 2 to contain the elastic properties of the cement paste which is the matrix phase in scale 3.. The elastic properties of the product of hydration and pozzolanic reactions were obtained from previous experimental studies [11, 16, 20, 21]. The inclusion phases considered spherical in shape are the unreacted clinker, crystallized products (C_4AH_{13}, C_3AH_6 and C_2ASH_8) and metakaolin [16,22]. Meanwhile, the inclusion phases considered spherical and ellipsoidal with different eccentricity were the CH and pore phases. The matrix phase is the CSH gel. For the hydration reaction, the volume fraction considered is obtained from an existing study [23]. For the pozzolanic reaction, the volume fractions are modeled based on the stoichiometric study of the said reaction. The reaction considered is the sum of the three equations proposed by Rojas and Cabrera[24].

$3AS_2 + 14CH + 18H \rightarrow 5CSH + C_4AH_{13} + C_3AH_6 + C_2ASH_8$ (33)

Table 2 shows the volume fractions of the products of the hydration reaction. It is worth noting that, only the hydration reactions of C_2S and C_3S are considered.

Table 2: Volume fractions of the products of the hydration reaction, where a, b, c, d, e and f are volume fractions of CSH gel, CH, pores, unreacted clinker, e the shrinkage, cement and g water, respectively.

	Reagents		Products			
Elements	Cement	Water	CSH	CH	Pore	Clinker
Volume fractions	F	G	$\frac{a}{1-e}$	$\frac{b}{1-e}$	$\frac{c}{1-e}$	$\frac{d}{1-e}$

Table 3 shows the stoichiometric volume fraction of the products of the pozzolanic reaction, in which a_1 is the volume fraction of CH reacting with the available metakaolin added, b_1 the volume fraction of metakaolin added, c_1 volume fraction of water from pore used in the pozzolanic reaction, a_2 the volume fraction of CSH gel, b_2 volume fraction of C2ASH8, c_2 the volume fraction of C3AH6 and d_2 the volume fraction of C4AH13, with

$$\mu = \frac{1}{1-e+c_{mk}f},\ \beta = \frac{1}{a_2+b_2+c_2+d_2}\left(1+\frac{a_1}{b_1}+\frac{c_1}{b_1}\right). \quad (34)$$

Given that we used weight fraction of metakaolin, n_{mk}, with respect to the mixture of cement and metakaolin in our experimental measurements, we will need to express this weight fraction as a volume fraction, c_{mk},

$$c_{mk} = \frac{\rho_{cement}}{\rho_{mk}\left(\frac{1}{n_{mk}}-1\right)+\rho_{cement}} \quad (35)$$

Table 3: Volume fraction of the product of the pozzolanic reaction with respect to the total volume of concrete.

	Reagents			Products			
Elements	CH :	MK :	water:	CSH	C_2ASH_8 :	C_3AH_6 :	C_4AH_{13} :
Volume fractions	$\frac{a_1}{b_1}c_{mk}f\mu$	$c_{mk}f\mu$	$\frac{c_1}{b_1}c_{mk}f\mu$	$c_{mk}f\mu a_2$	$c_{mk}f\mu b_2$	$c_{mk}f\mu c_2$	$c_{mk}f\mu d_2$

It is assumed that there is no change in volume during the pozzolanic reaction. The quantity of metakaolin necessary to react with all the experimentally known quantity of CH available, $b\mu$, is given by $\frac{b_1}{a_1}b\mu$. Expressing this quantity in terms volume fraction with respect to the volume of cement leads by accounting to the second box of Fig.3 to:

$$c_{mk} = \frac{b_1}{a_1}\frac{b}{f}. \quad (36)$$

Two possible situations arise:

- For $c_{mk} \le \frac{b_1}{a_1}\frac{b}{f}$, the quantity of metakaolin added is less than or equal to the quantity needed to react with all available CH. The inclusion phases are the C_4AH_{13}, C_3AH_6, C_2ASH_8, pore, clinker and surplus CH. The matrix phase is the CSH gel. The volume fractions are:

$$c_{CSH} = a\mu + c_{mk}f\mu a_2\beta, \quad (37)$$

$$c_{CH} = \mu\left(b\mu - c_{mk}f\frac{a_1}{b_1}\right), \quad (38)$$

$$c_{pore} = \mu\left(c\mu - c_{mk}f\frac{a_1}{b_1}\right). \quad (39)$$

Let us assume that the quantity of water needed in the pozzolanic reaction comes from the pores. Therefore, the additional volume of product obtained will occupy the pores volume previously occupied by water, leading to

$$c_{clinker} = d\mu, \quad (40)$$

and then

$$c_{C_2ASH_8} = c_{mk}fb_2\mu\beta, \quad c_{C_3AH_6} = \frac{c_2}{b_2}c_{C_2ASH_8},\ c_{C_4AH_{13}} = \frac{d_2}{b_2}c_{C_2ASH_8}. \quad (41)$$

- When $c_{mk} > \frac{b_1}{a_1}\frac{b}{f}$, the quantity of metakaolin added is more than the quantity needed

to react with all the CH available. The inclusion phases are the C_4AH_{13}, C_3AH_6, C_2ASH_8, pore, clinker and surplus metakaolin. The matrix phase is the CSH gel. The volume fractions are then

$$c_{AS_2} = \left(c_{mk}f - b\frac{b_1}{a_1}\right)\mu,\ c_{pore} = \mu\left(c - \frac{c_1}{a_1}b\right), \quad (42)$$

$$c_{clinker} = \frac{d}{1-e+c_{mk}f}, \quad (43)$$

$$c_{C_2ASH_8} = b\mu b_2\beta, \quad c_{C_3AH_6} = \frac{c_2}{b_2}c_{C_2ASH_8},\ c_{C_4AH_{13}} = \frac{d_2}{b_2}c_{C_2ASH_8}. \quad (44)$$

3.3 Scale 3:

The self-consistency scheme was applied for model 1 and the Mori-Tanaka scheme is applied for model 2 to obtain the elastic properties of mortar which is the matrix phase in scale 4. The matrix phase is cement paste. The inclusion phases are sand and void. The sand inclusion is considered spherical while the void phase is considered spherical and ellipsoidal with different eccentricity. The elastic properties of sand are obtained from a previous study [15]. The volume fractions of sand and cement phases are obtained from the concrete formulation [6] as done in previous studies [11]. The volume fraction of void is obtained from an existing experimental study [25]

3.4 Scale 4:

The Self-consistency scheme was applied for model 1 and the Mori-Tanaka scheme is applied for model 2 to obtain

the elastic properties of concrete. The matrix phase is mortar. The inclusion phases are the small and coarse gravel. The small and coarse gravel inclusions are considered spherical and ellipsoidal with various eccentricities. The elastic properties of small and coarse gravel are obtained from an existing study [9]. The volume fractions of the phases are obtained from the formulation of concrete. The two models are simulated in MATLAB and Young's modulus obtained from the effective stiffness tensor calculated. Finally, graphs of Young's modulus for various percentage of substitution of metakaolin are plotted.

3.5. Experimental measurement

Twelve samples were studied such that two samples were used for each rate of substitution of cement with metakaolin. The mixture properties, the sample designation and the average Young modulus measured are outlined in Table 4. Cylindrical specimens of radius 10cm and height 20cm were used for each sample. The three-point bending experiment was conducted on each sample and the Young modulus deduced. BK 0, BK7.5, BK10, BK12.5, BK15 and BK17.5 have 0%, 7.5%, 10%, 12.5%, 15% and 17.5% of substituted cement with metakaolin respectively. The kaolin used has the chemical composition as given in Table 5.

Table 4: Mix ratios and experimental measurements.

Sample designation	Sample number	Tensile strength (kN)	Young modulus (MPa)	Mass per unit volume in kg/m^3					
				Cement	Metakaolin	Coarse gravel, 15/25	Fine gravel, 5/15	sand	Slump (mm)
BK 0	Sample 1	201.7	27654.29424	350	0	481	699	647	120
	Sample 2	206.3							
BK 7.5	Sample 3	245.7	30155.31613	323.75	26.25	481	699	647	95
	Sample 4	241.3							
BK 10	Sample 5	264.4	30901.87498	315	35	481	699	647	83
	Sample 6	269.2							
BK 12.5	Sample 7	254.4	30533.22816	306.25	43.75	481	699	647	71
	Sample 8	249.2							
BK 15	Sample 9	238.3	29767.53574	297.5	52.5	481	699	647	68
	Sample 10	238.3							
BK 17.5	Sample 11	232.8	29369.21852	288.75	61.25	481	699	647	46
	Sample 12	232.4							

Table 5: Chemical composition of kaolin clay (L.F. = loss on fire).

Oxides	SiO_2	Al_2O_3	Fe_2O_3	TiO_2	K_2O	Na_2O	SO_3	V2O5	Cl	L.F.	Total
percentage	43,45	37,60	1,98	0,93	0,70	0,51	0,06	0,04	0,01	13,8	99,17

The kaolin clay was dried in an oven at 105 °C for 24 hours then crushed and dry sieved at 100 µm. It was later heated at 700 ^{0}C for 5 hours to obtain the metakaolin. Since, the main factor used to distinguish different metakaolins as supplementary cementious material is the S/A ratio [26], the chemical composition the metakaolin was sought by the X-ray fluorescence method using a Panalytical type spectrometer. The results found are presented in the Table 6.

Table 6: Chemical composition of metakalin (L.F. = loss on fire).

Oxides	SiO_2	Al_2O_3	Fe_2O_3	CaO	MgO	Na_2O	K_2O	TiO_2	MnO	P_2O_2	L.F.
percentage	56,58	21,81	9,26	0,03	0,03	0,10	0,74	1,95	0,01	0,15	3,11

Setting that the S/A ratio is 2.6 and since S/A ratio higher than 1.5 have been proven to have enhanced pozzolanic activity[27], it can concluded that the metakaolin used conforms to existing norms of pozzolanic activity. We can then conclude that the observation made in this work are valid for metakaolin with high pozzolanic activity.

4. Results

This section presents results about values of the Young modulus (YM) of concrete as elastic property for various shapes of inclusions involved in function of the rate of metakaolin added. Numerous arrangements of shapes are then taken into account. Figures 2 and 3 depict the predicted YM (In blue line) obtained by solving numerically the set of Equations 3, respectively for model 1 (spherical in shape) and model 2 (ellipsoidal and spherical in shape), while in the same figures (black line), one has the YM obtained experimentally. The curves obtained by

taking into account the errors $\pm 10\%$ of experimental YM are shown in red dashed line. As one can see, for model 1 (see Fig. 2) the curves of experimental and predicted YM are close to one another, far below the allowable error. It is worth noting that in the band $[0; 4] \cup [10; 18[$ the predicted YM are lower than the experimental one, and in the interval $[4; 9]$ the predicted YM are higher than that found experimentally. At about 4% and 18% the predicted YM is almost equal to the experimental one. Otherwise, the predicted YM and experimental one is nearly equal for the rate of metakaolin added belonging to $[0; 8.5] \cup [12; 18]$. Then, model 1 involving the self-consistency scheme predicts values closed to experimental observations. But, the prediction of the peak values is different from the experimentally observed ones and always at lower rate of substitution.

For the second model as shown in Fig.3, the experimental and predicted YM have nearly the same shape for the rate of metakaolin $\leq 9\%$. The predicted values are almost identical to the experimental one in the interval [6; 9]. For all other rate of substitution, the predicted values are always lower than the experimental ones. While that predicted is nearly identical to that found experimentally, since $(1 - 10\%) \times (\text{Experimental YM}) \leq \text{Predicted YM} \leq (1 + 10\%) \times (\text{Experimental YM})$, which is in agreement with the results found by Zadeh and Bobko[11] for model 2 involving the Mori-Tanaka predicted. In some cases, values are closed to the experimental observations. In this shape arrangement, the elastic property predicted is closed to experimental values. These cases are found whether all the inclusion phases are considered spherical, that is when the void inclusion phase is considered ellipsoidal with ratio 9:3:1 and 4:2:1 in the x, y and z directions respectively. It should be noted that their predictions are very similar with the main difference of the increase in predicted values of Young modulus when the inclusion are ellipsoidal in shape. Moreover, both model 1 and 2 predictions of YM belonging in the interval [10; 18[are lower than the experimental one, showing that other factors may also contribute to the increasing of the YM above the optimal rate of substitution of metakaolin. But, the prediction of the peak values is different from the experimentally observed ones and always at lower rate of substitution. This difference is probably due to the difference between the optimal rate used in the model and the observed one since; it is assumed that all the metakaolin added chemically reacts. Another factor may be the fact that the hydration of C_3A and C_4AF are not taken into consideration.

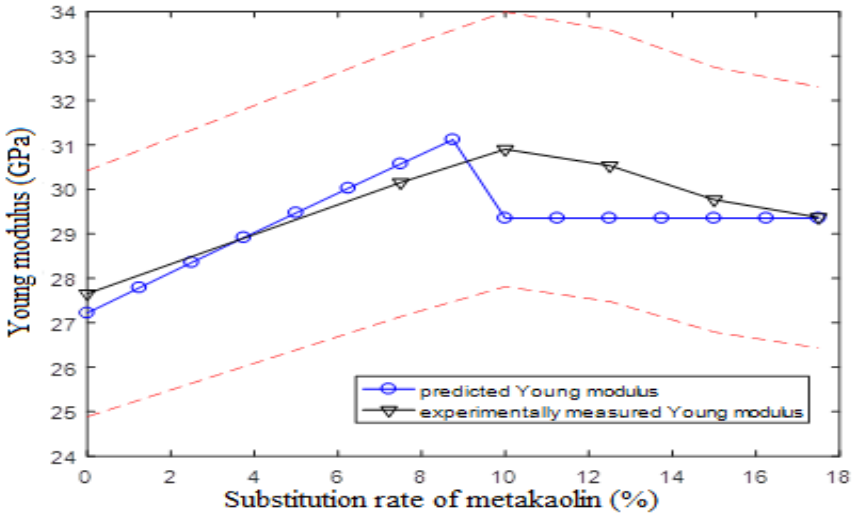

Fig. 2: Young modulus obtained for arrangement when all inclusion phases are spherical in shape for the first Model.

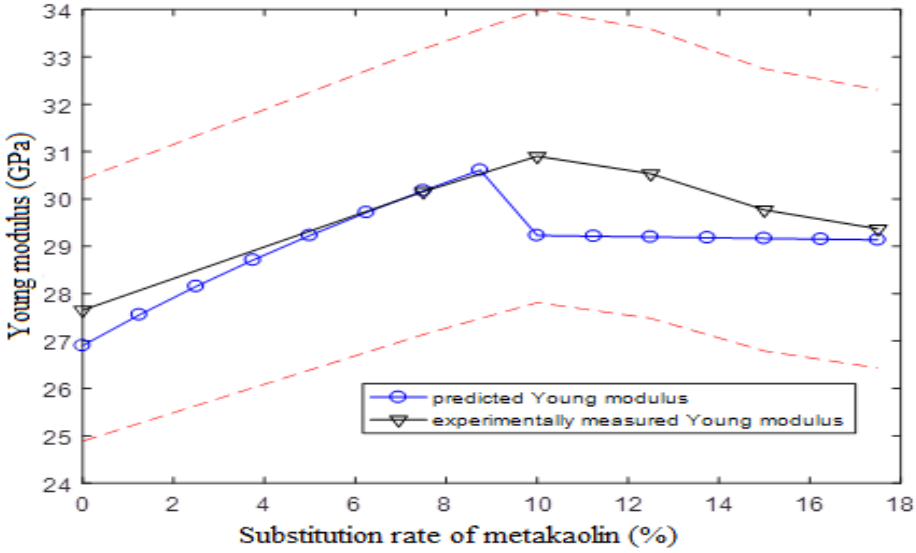

Fig. 3: Young modulus obtained for arrangement when all inclusion phases are ellipsoidal in shape for the second model

5. Conclusion

In this paper, four scales were used to predict the elastic properties of concrete with partial substitution of ordinary Portland cement with metakaolin, while two models were used involving both the self-consistency and Mori-Tanaka homogenisation schemes. The products of the pozzolanic reaction were taken into account, including the spherical and ellipsoidal shapes for some inclusions phases. The predictions were compared with experimental observations on ordinary concrete with metakaolin as partial substitute of CEM I, cement. Four of the considered possibilities had predictions, consistent with the experimental observations with the error of $\pm 10\%$. However, the prediction of the peak values was different from the experimentally observed ones and always at lower substitution rate, which is probably due to the difference between the optimal rate used in the model and the observed one, since it was assumed that all the metakaolin added chemically reacted, and some important factors such as the hydration of C_3A and C_4AF were not taken into consideration. In addition, there seem to be a factor that contributes to the increase of the YM above the optimal rate of substitution other than the pozzolanic reaction. It is important to mention that the results proposed in the present work could help engineers to predict numerically the young modulus of concrete whether they intent to partially substitute cements with locally available metakaolins.

References

1. Joaquín Abellán-García, María Alejandra Santofimio-Vargas, Nancy Torres-Castellanos,' Analysis of Metakaolin as Partial Substitution of Ordinary Portland Cement in Reactive Powder Concrete ', Advances in Civil Engineering Materials 9 (2020) 1
2. C. Deuteuf, "Procédé de fabrication de Métakaolin Imerys", séminaire géopolymères, pp1-7, 2012.
3. S. Wild, B.B. Sabir and J. Bai, "Metakaolin and calcined clays as pozzolans for concrete: A review, cement-concrete composites", Cement and concrete composites, volume 23, issue 6, pp441-45, 2001.
4. M. Antoni, J. Rossen, F. Martirena, K. Scrivener,' Cement substitution by a combination of metakaolin and limestone', Cement and Concrete Research 42 (2012) 1579–1589
5. C. Nitaa , V.M. Johna , C.M.R. Dias, H. Savastano and M.S. Takeashi, "Effect of Metakaolin on the presence of PVA and cellulose fibers reinforced cement", Researchgate , pp1-10, 2004.
6. N. K. Murthy, A.V.N. Rao, M.V.S. Reddy and P.Pamesh, "The influence of metakaolin on the modulus of elasticity of concrete", IOSR journal of engineering, volume 2, pp18-23, 2012.
7. A. Jehma, S. U. Khan and F. A. Memon "Mechanical characteristics of hardened concrete with different mineral admixtures", the Scientific World Journal, volume 2014, pp1-14, 2014.
8. M. M. Ashik and D. Gomathi, "Strength properties of concrete using metakaolin" International Journal of Engineering Research & Technology (IJERT) , vol. 6 issue 11, pp141-151, 2017.
9. A. A. Amer, D. Hamdy, T.M. Sokkary et H. Samir, "Hydration and characteristics of Metakaolin pozzolanic cement pastes", NBRC journal, volume 14, issue 3, pp181- 197, 2019.
10. G. Constantinides, F.J. Ulm, F.J. Heukamp Emílio and C.C.M. Silva, " [Bio-] Chemo mechanical at finer scales- A review", Materials and structure, volume 36, pp5-8, 2003.
11. Z. Zadeh et C. P. Bobko, "Multiscale modelling of elastic properties of sustainable concrete by microstructural-Based micromechanics", Journal of composites, volume 2014, pp1-9, 2014.
12. Christian Pichler, Roman Lackner, Herbert A. Mang,' A multiscale micromechanics model for the autogenous-shrinkage deformation of early-age cement-based materials', Engineering Fracture Mechanics 74 (2007) 34–58
13. M.L. Nazargah, S.A. Emamian, E. Aghasizadeh and M. Khani, "Predicting the mechanical properties of ordinary concrete and nano-silica using micromechanics", SADHANA, volume 46, pp 1-10, 2018.
14. Tchapga Gnamsi Guy, Molaya Mambou Ngueyep Luc Leroy, Tchoffo Fidele, Hamidou Gilbert Franck, Ndjaka Jean-Marie Bienvenu,'Mechanical and physical performances of concretes made from crushed sands of different geological nature subjected to high temperatures', Engineering Science and Technology, an International Journal 22, 4 (2019) 1116-1124
15. H. Mazaheripour, R. Faria and M. Azenha "Microstructure-Based prediction of elastic behavior of hydrating cement paste", Cement and concrete composites, volume 36, pp2-9, 2018.
16. G. Constantinide et J. T. Jeffrey., "Nanostructure of CSH gel in cement paste as a function of curing conditions and relative humidity", Cement and concrete composites, pp1-15, 2005.
17. G. Dvorak, "Micromechanics of composite materials", Waterloo, Solid mechanics and application, volume 185, pp1-217, 2013.
18. Q. Jiamin et C. Mohammed, "Fundamentals of micromechanics of solids", new jersey, John Wiley & Sons, first edition, pp154-214, 2018.
19. M. Dutta, L. Debnath, Elements of the Theory of Elliptic and Associated Functions with Applications, World Press Pub. Ltd., Calcutta (1965)
20. Y. Yoda, S. Krishnya and Y. Elakneswaran, "A two stage model for prediction of mechanical properties of cement paste", Cement and concrete composites, pp2-6, 2021.
21. C. J. Haecker, E. J. Garboczi, J. W. Bullard, R. B. Bohn, Z. Sun, S. P. Shah and T. Voig, "Modelling the linear elastic properties of Portland cement paste", Cement and concrete research, pp1950, 2007.
22. J. L. Lawson, "On the determination of the elastic properties of geopolymers materials using non-destructive ultrasonic techniques", thesis, pp40-56, 2008.
23. O. Cize, V. Balen, K. Gemert and D.E. Jan, "Carbonation and hydration of mortars with hydroxide and calcium silicate binders", International Conference on Sustainable Construction Materials and Technologies, pp. 611 – 621, 2007.
24. F. Rojas and J. Cabrera, "The effect of temperature on the hydration rate and stability of the hydration phases of Metakaolin-lime-water system", Cement and concrete research, volume 32, pp133-138, 2012.
25. P. C. Fonseca and G. W. Scherers, "An image analysis

procedure to quantify the air void system of mortar and concrete", pp3090-3095, 2015.
26. A. S. Rinuu, "Synthesis of metakaolin-based geopolymer and its performance as sole stabilizer of expansive soils", PhD thesis, University of texas, pp 36 - 39, 2019.
27. P. Sungwoo, Y. Juan, E. Jae and P. Sukhoon, "Efect of Silica Fume on the Volume Expansion of Metakaolin-Based Geopolymer Considering the Silicon-to-Aluminum Molar Ratio", International Journal of Concrete Structures and Materials, pp 1-2, 2022.